



Modifications in structural, morphological and optical properties of TiO₂ nanoparticles: effect of pH

Shweta Manchwari¹ · Jaya Khatter¹ · R. P. Chauhan¹

Received: 29 May 2022 / Accepted: 16 August 2022 / Published online: 25 August 2022
© Institute of Chemistry, Slovak Academy of Sciences 2022

Abstract

Titanium dioxide (TiO₂) is an exclusive system to study the nanoscale phenomenon due to its unique optical and electrical properties and, also, for its promising future applications. In this paper, three different samples of TiO₂ are synthesized using different acidic concentrations in synthesis reaction, and subsequently, comparison has been made among them. Hydrothermal method is used for synthesis of TiO₂ nanoparticles and nitric acid (HNO₃) is utilized for controlling the acidic concentration. Characterization techniques like X-ray diffraction (XRD), scanning electron microscopy (SEM), UV–visible spectroscopy and photoluminescence (PL) spectroscopy are employed to study the structural, morphological and optical properties of resulting nanoparticles. XRD analysis shows that increase in HNO₃ concentration resulted into enlargement in size of TiO₂ nanoparticles. Hydrothermally synthesized nanoparticles showed different morphologies (i.e., nanoflakes, nanotubes, and nanoparticles) at different concentrations. Also, the band gap energy of samples is affected by the change in acidic concentrations wherein TiO₂ nanoparticles of smallest size exhibit the largest band gap when compared with other two.

Keywords Titanium dioxide · Hydrothermal · pH · Optical properties

Introduction

In recent times, nanomaterials-based research has got huge attention due to their distinctive and impressive optical and electrical characteristics as compared to their bulk counterparts. Nanomaterials provide extensive information about optical and electronic structure using optical methods. Semiconducting nanocrystalline materials offer potential applications in various fields like heterogeneous photocatalysis, sustainable energy, nonlinear optics, etc. One such material gaining wide interest among researchers is titanium dioxide (TiO₂). TiO₂ first gained attention in 1972 after Fujishima discovered photolysis of water on crystal titania (TiO₂) electrode (Wahyuningsih et al. 2014). It basically exists in three forms: rutile, anatase

and brookite. Among these, anatase is being studied more than the other two as it offers indirect band gap whereas rutile and brookite belong to direct band gap semiconductor category. The unique properties of TiO₂ include its chemical and biological inertness, stability, abundance, non-toxicity, cost effectiveness and high photocatalytic activity (Verbruggen et al. 2014). TiO₂ has gained immense amount of attention for its photocatalytic activities, as it has tremendous potential for such applications as in environmental refinement, carbonic acid gas (H₂CO₃) decomposition, and hydrogen gas generation (Binas et al. 2017; Dhayal et al. 2007). However, TiO₂ has two major drawbacks: its large band gap and its high recombination rate. These drawbacks limit its photocatalytic activities to UV region only. Many efforts have been aimed for acquiring the TiO₂ nanoparticles with high performance and large surface area. Controlling the size of semiconducting nanoparticles and, consequently, their physical and chemical properties is a crucial issue to probe the novel properties of materials in nanotechnology. There are various methods utilized for preparation of TiO₂ nanoparticles including hydrothermal method (Azeez et al. 2018), sol gel method (Azeez et al. 2018), solvothermal method (Moura et al. 2014), etc. These synthesis methods are capable to

✉ R. P. Chauhan
chauhanrpc@gmail.com

Shweta Manchwari
m9299755@gmail.com

Jaya Khatter
jayakhat2@gmail.com

¹ Department of Physics, National Institute of Technology, Kurukshetra 136119, India

provide TiO_2 particles of very small size, even in hundreds of nanometers. Among these methods, hydrothermal method is a low temperature technique used for controlled growth of nanocrystalline titania particles and is broadly accepted for industrial synthesis of ceramics. It depends on ample heating of nanoparticles mixed over an aqueous solution and requires an autoclave setup for the process. Hydrothermal method, being solution based, minimizes the tedious paste preparation steps by dissolving needed reagents before heating, promising flexibility in the procedure. Thus, TiO_2 nanoparticles are anticipated to be easily produced and to be offering qualities like stability, adherence and high photocatalytic activity (Zhang et al. 2002).

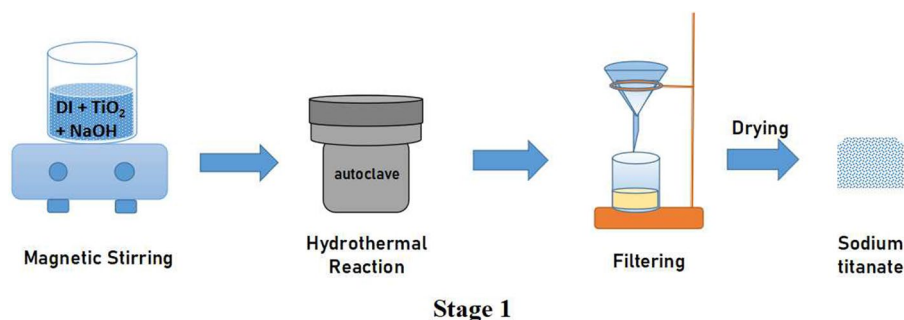
Different parameters such as reaction time, reaction temperature, calcination temperature, and reaction pH affect the different properties of TiO_2 like morphology, optical and electronic characteristics. Seo et al. treated TiO_2 nanoparticles at different hydrothermal temperatures and witnessed phase transformations at different temperatures (Seo et al. 2008). The pH variation is one of the most important aspects to study the properties and capabilities of TiO_2 . Nasikhudin et al. showed that the photocatalytic activities show variations when the medium changed from acidic to neutral to basic (Nasikhudin et al. 2018). In the present work, we have synthesized TiO_2 nanoparticles via hydrothermal route at different pH conditions where HNO_3 in the solution reaction is used as the basis of pH study. Changes in structural properties along with change in band energy have been witnessed at different acidic concentrations, which are studied and evaluated using characterization techniques.

Experimental details

Chemicals used

Titanium dioxide (TiO_2) powder (98% pure), sodium hydroxide (NaOH) pellets (97% purity), acetone, deionized (DI) water, and nitric Acid (HNO_3) are procured and used as obtained without additional refinement.

Fig. 1 Formation of Sodium-Titanate



Synthesis

Synthesis process used in this paper is basically divided into three parts:

In stage 1, 10 M of NaOH pellets are dissolved in 80 mL of DI water under magnetic stirring for 30 min. Then, 2 g of TiO_2 is added into the solution and the resultant solution is stirred for 1 h to get uniform and homogenous solution (Fig. 1). The resulting solution is placed in hydrothermal reactor for 20 h at 200 °C in 100 mL Teflon lined stainless steel autoclave. After cooling at ambient temperature, sample is filtrated and washed several times with large amount of DI water and, then, put for drying at 80 °C for 12 h. The sample is then grinded with mortar pestle to obtain sodium titanate.

In stage 2, resulting powder then suspended in 0.1 M HNO_3 and put for magnetic stirring for 6 h. Finally, the resulting solution is filtered and washed repeatedly with ethanol and DI water until pH became neutral and, then, put for overnight drying at 80 °C for 12 h. (Fig. 2).

In stage 3, resulting sample from stage 2 is suspended in different concentrations of HNO_3 and, then, transferred into next hydrothermal treatment at 200 °C for 20 h. After that, it is filtered and dried out for 12 h. Further, sample is grinded in mortar pestle to obtain uniform powder sample. Different concentrations of HNO_3 are used in this paper for pH study. This reaction process is illustrated in Fig. 3. The final product obtained is labeled as TiO_2 -1, TiO_2 -2 and TiO_2 -3 for concentrations of HNO_3 of 10^{-4} M, 10^{-2} M and 10^{-1} M in second hydrothermal process.

Characterization

The powder X-ray diffraction (XRD) is performed using Rigaku Miniflex II X-ray diffractometer with an incident Ni-filtered $\text{Cu K}\alpha$ radiation ($\lambda = 1.54 \text{ \AA}$). Scanning electron microscopy (SEM) is done using JEOL JSM-6390 JV scanning electron microscope (SEM) for studying the size of synthesized product and its morphology. FTIR characterization is carried out using the BRUKER spectrophotometer for analysis of functional groups in the sample. The UV–vis

Fig. 2 Midway process for formation of Titanium nano-structures

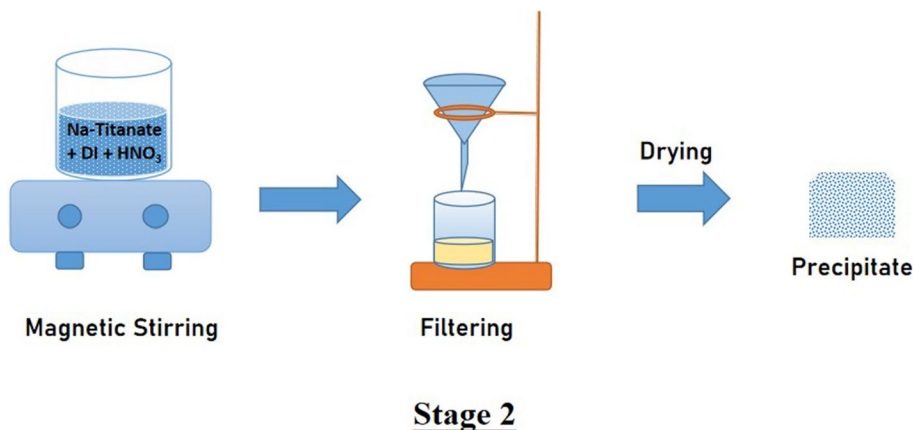
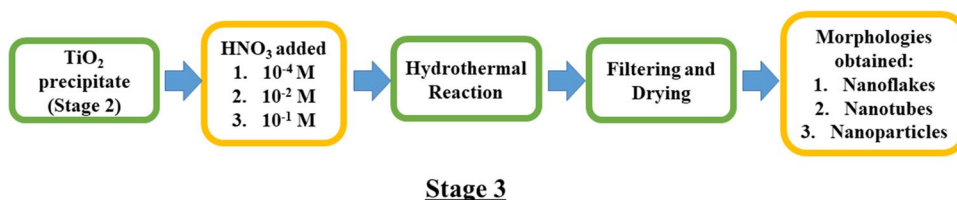


Fig. 3 TiO₂ morphologies based on different pH values



absorption spectrum is recorded with the help of UV–visible Lambda 650 Spectrophotometer (PerkinElmer), and photoluminescence (PL) spectrum is noted at room temperature using SHIMADZU RF-530 Spectrofluorometer with a Xe lamp for the analysis of optical properties.

Results and discussion

X-Ray diffraction (XRD)

Figure 4 represents the XRD characterization for TiO₂ nano-structures prepared at various acidic concentrations. The peaks at 25.35°, 36.9°, 37.9°, 38.5°, 47.9°, 53.9°, 62.04°, 62.65°, 68.6°, 70.2° and 75.02° can be attributed to the (101), (103), (004), (112), (200), (105), (211), (204), (116), (220) and (215) which corresponds to the crystal phase of the anatase structure (JCPDS No. 894921). This graph shows that the peak intensity increases with the concentration of HNO₃ in the final product. The intense and sharp diffraction peaks indicated its crystalline structure in TiO₂-2 and TiO₂-3. The broad peaks suggest that the particles are semi-crystalline in nature or are of very small crystalline size (Yeh et al. 2004). We can also conclude that TiO₂-1 had broader peaks than TiO₂-2 and TiO₂-3, notifying its smaller size than the other two. Similarly, TiO₂-2 was smaller in size than TiO₂-3, as it is showing broader peak when compared to another. The crystallite size of the TiO₂ nanostructures

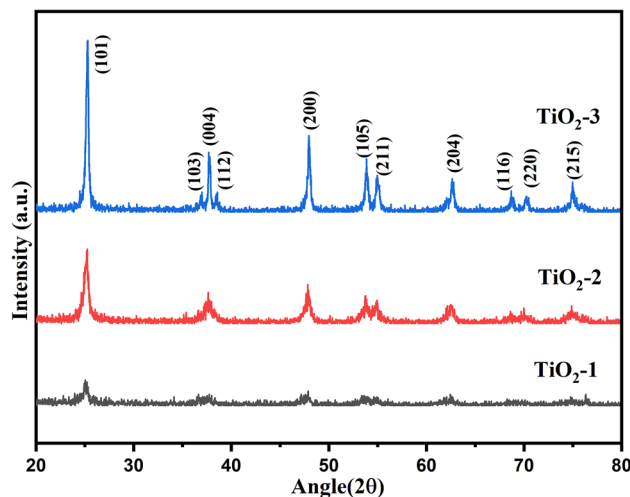


Fig. 4 XRD pattern for **a** TiO₂-1 (10⁻⁴ M HNO₃); **b** TiO₂-2 (10⁻² M HNO₃); and **c** TiO₂-3 (10⁻¹ M HNO₃)

is determined using Debye's Scherer equation (Mustapha et al. 2021);

$$D = 0.9 \lambda / \beta \cos \theta \quad (1)$$

where D is the crystallite size, λ is the wavelength of X-ray, θ is the Bragg's angle in radians, and β is the full width at half maximum of the peak in radians. Crystallite size for TiO₂-1, TiO₂-2 and TiO₂-3 is found to be 6 nm, 11 nm and 20 nm.

The synthesized TiO₂ nanostructures are of tetragonal phase with the lattice constants $a = b = 3.7$ and $c = 9.5$.

Scanning electron microscopy (SEM)

SEM images for as-synthesized samples are illustrated in Fig. 5a–c. It is observed that morphologies of obtained sample are affected by the pH of solution. As the acidic concentration increased from TiO₂-1 to TiO₂-2 to TiO₂-3, the resulting structures changed from nanoflakes (Fig. 5a) to nanotubes (Fig. 5b) to irregular shaped nanoparticles (Fig. 5c). Increase in pH resulted into the agglomeration in resulting samples, which can be mainly due to electrostatic repulsive forces or Van der Waals attractive forces. In hydrothermal formation of TiO₂ nanoparticles in concentrated NaOH aqueous solution (in step a), it is found that the resultant samples are sensitive to acid. Xu et al. (Xu et al. 2010) also noticed the same behavior in his study where he got the formation of nanoparticles from nanotubes occurring at higher acidic concentration. From these results, it can be deduced that pH plays a significant role in controlling the morphologies of nanostructures.

Fourier transform infrared spectroscopy (FTIR)

FTIR is a preferred method of infrared (IR) spectroscopy. FTIR spectrum for obtained sample denotes the molecular absorption and transmission, which can be used for creating the molecular fingerprint of the sample. Figure 6

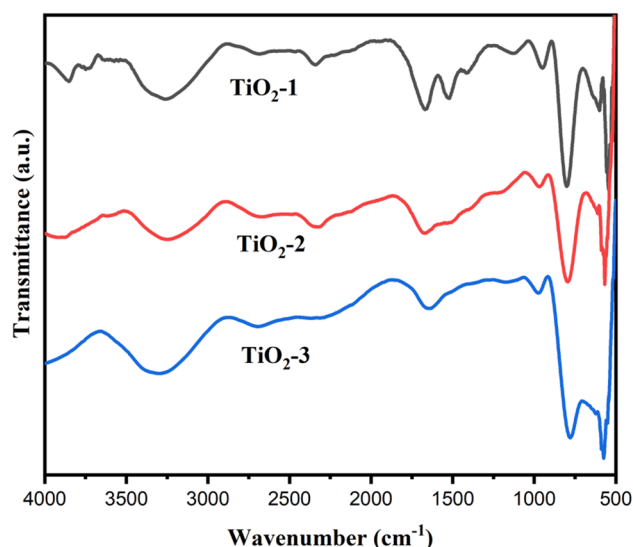
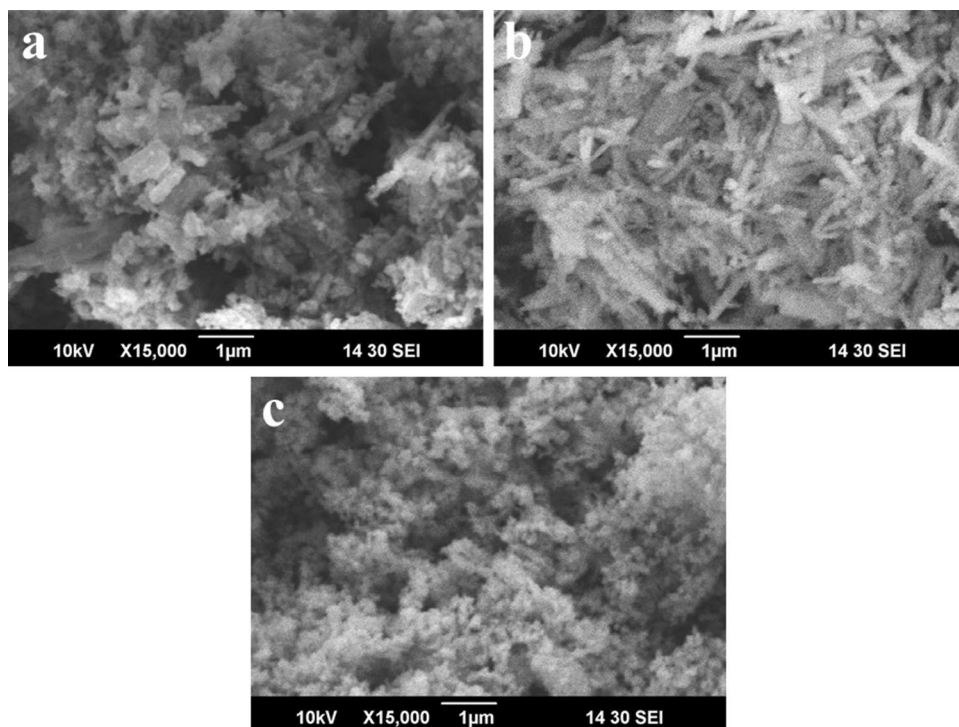


Fig. 6 FTIR characterization of TiO₂

represents the FTIR spectrum for the synthesized sample. The sharp bands from 500–1000 cm⁻¹ can be assigned to Ti–O bonding (Tabbiche & Aouinti., 2022), where the peak near 650 cm⁻¹ is due to Ti–O bonding and the peak near 800 cm⁻¹ is present because of the O–Ti–O bonding (Khan et al. 2021). The peak present at 1662 cm⁻¹ can be related to the water molecule bending mode (Tripathi et al. 2013) and the corresponding band from 3000–3550 cm⁻¹ represents the interacting hydroxyl groups which attributed in

Fig. 5 SEM characterization for a TiO₂-1; b TiO₂-2; and c TiO₂-3



hydrogen bonding and molecular water coordinated to Ti^{4+} ions (Govindhan and Pragathiswaran., 2016). With increasing acidic concentration, decrease in peak intensities is witnessed suggesting that the amount of functional group associated with the molecular bond is decreasing in the order: $\text{TiO}_2\text{-1} > \text{TiO}_2\text{-2} > \text{TiO}_2\text{-3}$ (Simonescu, 2012).

Photoluminescence spectroscopy (PL)

Figure 7 shows the PL spectra for as-synthesized TiO_2 nanoparticles at the excitation wavelength of 325 nm. The excitation wavelength of 325 nm is analogous to the band gap energy of 3.81 eV which is greater than the band gap of TiO_2 (approx. 3.2 eV). This energy is used to excite the valence electrons in the conduction band. In Fig. 7, all three samples of TiO_2 showed three peaks at wavelengths of 407 nm, 433 nm and 461 nm where the highest peak is observed at 433 nm that are assigned to band gap of 2.8 eV. Presence of multiple peaks in the given spectrum denoted the existence of defect levels in the band gap which is formed due to oxygen vacancies during sample preparation. High surface to volume ratio in TiO_2 nanoparticles also favored the existence of large quantities of oxygen vacancies (Zhao et al. 2007). Here, PL intensity decreased from $\text{TiO}_2\text{-2}$ to $\text{TiO}_2\text{-3}$ to $\text{TiO}_2\text{-1}$. Decrease in PL intensity indicated efficient electron hole separation and long-lived carriers (Yao et al. 2016). However, PL characterization for semiconductors at ambient temperature is not very accurate due to many factors like surface states and bulk defects that influence the fluorescence signals. Due to this, band gap obtained from PL spectra showed some variations from original band gap. However, electronic structure and state distribution can be correctly specified from these characterization results. Luminescence plots for all samples in excitation wavelength of

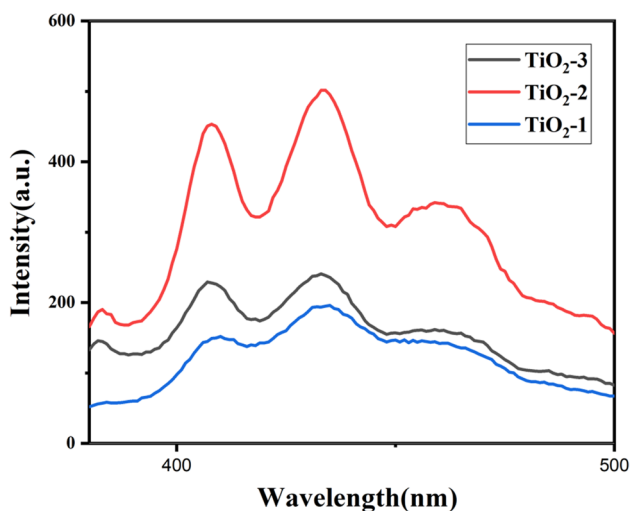


Fig. 7 PL Characterization of TiO_2 nanostructures

325 nm are almost identical, suggesting that the electronic state distributions of all samples within the energy band are similar.

UV-Vis spectroscopy

UV-visible spectroscopy is employed for the as-synthesized TiO_2 nanoparticles as shown in Fig. 8. The band gap energy of each sample is estimated based on Tauc and Menth's equation:

$$(Ah\nu)^n \propto h\nu - E_g \quad (2)$$

where A represents the absorbance, $h\nu$ represents the energy of the light; n is a constant equal to $1/2$ since anatase TiO_2

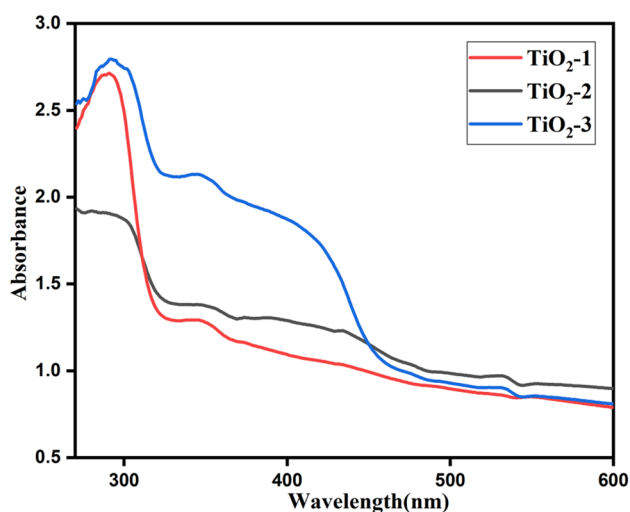


Fig. 8 UV-vis characterization of TiO_2 samples

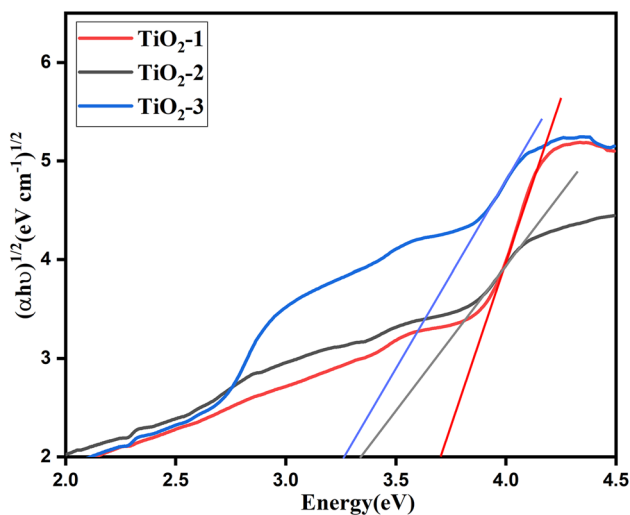


Fig. 9 Tauc plot for corresponding UV-Vis characterization

is indirect semiconductor, and E_g is the band gap energy determined by extrapolating the linear portion to $(Ah\nu)^{1/2}$ versus $h\nu$ (Fig. 9). From this graph, the band gap energy is calculated to be 3.7 eV, 3.3 eV and 3.2 eV for samples TiO₂-1, TiO₂-2 and TiO₂-3, respectively. Due to quantum size effect of TiO₂ nanoparticles, we observe a systematic blue shift in the absorption edge with the decrease in particle size. It is concluded that with decreasing particle size, the energy gap of TiO₂ is increasing and the electronic level spacing which is mainly due to the fact that the electron hole pairs are now much closer so that the columbic interaction in between couldn't be neglected giving an overall kinetic energy (Stroyuk et al. 2005).

According to the already existing literature (Akpan & Hameed, 2009; Guillard et al. 2003), the photocatalytic activities are reported to be increased with decreasing acidic concentrations. This study suggests the better potential photocatalyst can be given by order: TiO₂-1 > TiO₂-2 > TiO₂-3.

Conclusion

In the present study, we prepared three samples using hydrothermal method with different concentration of HNO₃ for their synthesis. In these processes, TiO₂-1 has lowest acidic concentration of 10⁻⁴ M, TiO₂-2 has medium acidic concentration of 10⁻² M and TiO₂-3 has the highest acidic concentration among them of 10⁻¹ M. All samples showed different morphological and optical properties. From the analysis, it is realized that the size of TiO₂ nanostructures decreased with decrease in the acidic concentration as depicted in XRD analysis. From SEM images, we are able to observe that the morphology changed from nanoflakes to nanotubes to nanoparticles with different concentration of HNO₃. Also, from absorption and luminescence spectroscopy, it is concluded that the band gap of TiO₂ nanoparticles increased with decrease in size which is due to the confinement of electrons and holes in the sample. This analysis suggested the effective utilization of TiO₂ nanoparticles for photocatalytic activities in terms of environmental purification by altering their properties with different amount of pH as TiO₂-1 with least acidic concentration can be stated as a potential photocatalyst in this comparison study.

Acknowledgements One of the authors (Shweta Manchwari) acknowledges the Director, NIT, Kurukshetra, for financial assistance in the form of fellowship. The authors also extend their warm gratitude to the Department of Physics at NIT, Kurukshetra, for the laboratory and characterization facilities.

Declarations

Conflict of interest The authors declare that they have no known competing financial interests or personal relationships that could have appeared to influence the work reported in this paper.

References

- Akpan UG, Hameed BH (2009) Parameters affecting the photocatalytic degradation of dyes using TiO₂-based photocatalysts: a review. *J Hazard Mater* 170:520–529. <https://doi.org/10.1016/j.jhazmat.2009.05.039>
- Azeez F, Al-Hetlani E, Arafa M et al (2018) The effect of surface charge on photocatalytic degradation of methylene blue dye using chargeable titania nanoparticles. *Sci Rep* 8(1):1–9. <https://doi.org/10.1038/s41598-018-25673-5>
- Binas V, Venieri D, Kotzias D, Kiriakidis G (2017) Modified TiO₂ based photocatalysts for improved air and health quality. *J Mater* 3(1):3–16. <https://doi.org/10.1016/J.JMAT.2016.11.002>
- Dhayal M, Jun J, Gu HB, Hee Park K (2007) Surface chemistry and optical property of TiO₂ thin films treated by low-pressure plasma. *J Solid State Chem* 180(10):2696–2701. <https://doi.org/10.1016/J.JSSC.2007.06.037>
- Govindhan P, Pragathiswaran C (2016) Synthesis and characterization of TiO₂@SiO₂-Ag nanocomposites towards photocatalytic degradation of rhodamine B and methylene blue. *J Mater Sci: Mater Electron* 27(8):8778–8785. <https://doi.org/10.1007/s10854-016-4902-x>
- Guillard C, Lachheb H, Houas A et al (2003) Influence of chemical structure of dyes, of pH and of inorganic salts on their photocatalytic degradation by TiO₂ comparison of the efficiency of powder and supported TiO₂. *J Photochem Photobiol, A* 158:27–36. [https://doi.org/10.1016/S1010-6030\(03\)00016-9](https://doi.org/10.1016/S1010-6030(03)00016-9)
- Khan TT, Rafiqul Bari GAKM, Kang HJ et al (2021) Synthesis of N-doped TiO₂ for efficient photocatalytic degradation of atmospheric NO_x. *Catalysts* 11(1):1–13. <https://doi.org/10.3390/catal11010109>
- Moura KF, Maul J, Albuquerque AR et al (2014) TiO₂ synthesized by microwave assisted solvothermal method: Experimental and theoretical evaluation. *J Solid State Chem* 210(1):171–177. <https://doi.org/10.1016/J.JSSC.2013.11.023>
- Mustapha S, Tijani JO, Ndamitso MM et al (2021) Facile synthesis and characterization of TiO₂ nanoparticles: X-ray peak profile analysis using Williamson-Hall and Debye-Scherrer methods. *Int Nano Lett* 11:241–261. <https://doi.org/10.1007/s40089-021-00338-w>
- Nasikhudin DM, Kusumaatmaja A, Triyana K (2018) Study on Photocatalytic properties of TiO₂ nanoparticle in various pH condition. *IOP Publ.* <https://doi.org/10.1088/1742-6596/1011/1/012069>
- Seo HK, Kim GS, Ansari SG et al (2008) A study on the structure/phase transformation of titanate nanotubes synthesized at various hydrothermal temperatures. *Sol Energy Mater Sol Cells* 92(11):1533–1539. <https://doi.org/10.1016/J.SOLMAT.2008.06.019>
- Simonescu CM (2012) Application of FTIR spectroscopy in environmental studies. *Adv Asp Spectrosc* 29:77–86
- Stroyuk AL, Kryukov AI, Kuchmii SY, Pokhodenko VD (2005) Quantum size effects in semiconductor photocatalysis. *Theoret Exp Chem* 41(4):207–228. <https://doi.org/10.1007/s11237-005-0042-8>
- Tabbiche A, Aouinti L (2022) Preparation and characterization of nanocomposite membranes based on PVC/TiO₂ anatase for the separation of toluene/n-heptane mixtures via pervaporation. *Polym Bull.* <https://doi.org/10.1007/s00289-021-04062-5>
- Tripathi AK, Singh MK, Mathpal MC et al (2013) Study of structural transformation in TiO₂ nanoparticles and its optical properties. *J Alloy Compd* 549:114–120. <https://doi.org/10.1016/j.jallcom.2012.09.012>
- Verbruggen SW, Tytgat T, van Passel S et al (2014) Cost-effectiveness analysis to assess commercial TiO₂ photocatalysts for acetaldehyde degradation in air. *Chem Pap* 68(9):1273–1278. <https://doi.org/10.2478/s11696-014-0557-3>

- Wahyuningsih S, Purnawan C, Kartikasari PA, Praistia N (2014) Visible light photoelectrocatalytic degradation of rhodamine B using a dye-sensitised TiO₂ electrode. *Chem Pap* 68(9):1248–1256. <https://doi.org/10.2478/s11696-013-0476-8>
- Xu Y, Fang X, Xiong J, Zhang Z (2010) Hydrothermal transformation of titanate nanotubes into single-crystalline TiO₂ nanomaterials with controlled phase composition and morphology. *Mater Res Bull* 45(7):799–804. <https://doi.org/10.1016/J.MATERRESBULL.2010.03.016>
- Yao N, Huang J, Fu K et al (2016) Reduced interfacial recombination in dye-sensitized solar cells assisted with NiO: Eu³⁺, Tb³⁺ coated TiO₂ film. *Sci Rep* 6(1):1–9. <https://doi.org/10.1038/srep31123>
- Yeh CL, Yeh SH, Ma HK (2004) Flame synthesis of titania particles from titanium tetraisopropoxide in premixed flames. *Powder Technol* 145(1):1–9. <https://doi.org/10.1016/j.powtec.2004.04.042>
- Zhang YX, Li GH, Jin YX et al (2002) Hydrothermal synthesis and photoluminescence of TiO₂ nanowires. *Chem Phys Lett* 365(3–4):300–304. [https://doi.org/10.1016/S0009-2614\(02\)01499-9](https://doi.org/10.1016/S0009-2614(02)01499-9)
- Zhao Y, Li C, Liu X et al (2007) Synthesis and optical properties of TiO₂ nanoparticles. *Mater Lett* 61(1):79–83. <https://doi.org/10.1016/J.MATLET.2006.04.010>

Publisher's Note Springer Nature remains neutral with regard to jurisdictional claims in published maps and institutional affiliations.

Springer Nature or its licensor holds exclusive rights to this article under a publishing agreement with the author(s) or other rightsholder(s); author self-archiving of the accepted manuscript version of this article is solely governed by the terms of such publishing agreement and applicable law.